CAGE Code 63005

CLEEN II Short Inlet Flight Test Public Report

DOCUMENT NUMBER:	RELEASE/REVISION	RELEASE DATE
EDNS04000144008	**001**	**19 January 2023** For Document Release Use

FAA Continuous Lower Energy, Emissions and Noise (CLEEN) Technology Demonstration Program

CONTRACT NUMBER

DTFAWA-15-A-80012, Modification P00012

CONTENT OWNER:

Rolls-Royce Corporation, inc.

All revisions to this document must be approved by the content owner before release.

Approved for Public Release

Copyright © 2023 Rolls-Royce. All rights reserved.

Approved for Public Release. Copyright © 2018 Boeing. All rights reserved.

Document Information

Original Release Date 19 January 2023	Contract or CDRL Number DTFAWA-15-A-80012, Modification P00012
Approved for Public Release	

Authorization for Release

	19/01/2023		
AUTHOR:	Dimitris Arzoglou	63005	19 Jan 2023
	Dimitris Arzoglou	Org. Number	Date
	19/01/2023		
AUTHOR:		63005	19 Jan 2023
	Kuen-Bae Lee	Org. Number	Date
	19/01/2023		
APPROVAL:	Senior Technical Specialist – Fan Aerodynamics	63005	19 Jan 2023
	Mark Wilson	Org. Number	Date
	1/19/2023		
DOCUMENT RELEASE:	Brad J. Belcher	63005	19 Jan 2023
	Brad Belcher	Org. Number	Date

Copyright © 2023 Rolls-Royce. All rights reserved.

Approved for Public Release. Copyright © 2018 Boeing. All rights reserved.

Table of Contents

List of Figures 4
Acronym List 5
1 Background & Objectives 6
1.1 Introduction 6
1.2 The Short Inlet Collaboration 7
2 Apparatus 8
2.1 The Short and Baseline Inlets 8
2.2 Test Vehicle 9
2.3 FTB Installation 9
2.4 Instrumentation 11
3 Target Test Points and Overview of Test Flights 14
3.1 Test Points of Interest 14
3.2 Overview of achieved flight testing 15
4 Flight Test Results 16
4.1 Ground static crosswind and headwind 16
4.2 Take-off rotation 17
4.3 High Angle-of-Attack inlet distortion 19
4.4 Cruise performance 21
5 Conclusions 23

Approved for Public Release. Copyright © 2018 Boeing. All rights reserved.

List of Figures

Figure 1-1. Compact Nacelle Concept 6
Figure 1-2. Production and short inlet comparison ..... **Error! Bookmark not defined.**
Figure 2-1. Short (left) and baseline (right) inlet hardware 8
Figure 2-2 The FTB with the test vehicle in the no. 2 position 9
Figure 2-3 Side view comparison of Short (top) and Baseline (bottom) inlets installed on the FTB 10
Figure 2-4 Front view of Short (left) and Baseline (right) inlets showing the rakes, metal spinner tip telemetry transmitter, telemetry receiver aerial at 11 o'clock and P2T probe at 12 o'clock. 11
Figure 2-5 Close-up of an inlet rake 12
Figure 2-6 Close-up of axial arrays of static pressure tappings and kulites on the short (left) and baseline (right) inlets 13
Figure 2-7 By-pass duct rakes 13
Figure 4-1 Fan responses expressed in AF levels at 2F/3EO and 3F/6EO in ground static crosswind and headwind 16
Figure 4-2 MTO thrust take-off from Tucson International Airport during the 1st flight of the short inlet on the FTB, 2 July 2022 17
Figure 4-3 Comparison of short (top row) vs baseline inlet (bottom row) MTO thrust take-off test point peak inlet AoA during lift-off rotation measurements 18
Figure 4-4 Comparison of 1F/1EO response between short and baseline inlet during 74klbf MTO-equivalent take-off rotation 18
Figure 4-5 Comparison of short and baseline inlet pre- and post-separation inlet rake total pressure contours in the power-on approach to stall max inlet AoA maneuver 20
Figure 4-6 Comparison of 1F/1EO responses for short and baseline inlets during power-on approach to stall 20
Figure 4-7 Comparison of 1T/4EO response for short and baseline inlet during M = 0.3 wind-up turns at 15,500 feet 21
Figure 4-8 Comparison of short (top row) vs baseline (bottom row) inlet cruise test point measurements 22

Approved for Public Release. Copyright © 2018 Boeing. All rights reserved.

Acronym List

1EO	1st Engine Order
1F1EO	1st Flap 1st Engine Order fan blade resonance mode
2F3EO	2nd Flap 3rd Engine Order fan blade resonance mode
3F6EO	3rd Flap 6th Engine Order fan blade resonance mode
1T4EO	1st Torsion 4th Engine Order fan blade resonance mode
AF level	Amplitude-Frequency normalized fan blade stress levels
AoA	Angle of Attack
BPR	By-pass Ratio
DAS	Data Acquisition System
(F)OGV	(Fan) Outlet Guide Vanes
FTB	Flying Test-Bed
IRIG	Inter-range Instrumentation Group timecode
Mn	Flight Mach number
MTO	Max Take-off
LFPR	Low Fan Pressure Ratio
LP	Low Pressure (compressor)
N1	Fan mechanical rotational speed, usually expressed as % of a nominal rpm
NAI	Nacelle Anti-Icing
P2T2 probe	Total pressure and total temperature measurement probe in the engine inlet
P_T	Local total pressure
P_{20}	Freestream total pressure measured in the engine inlet using the P2T2 probe
sfc	Engine thrust-specific fuel consumption
TRU	Thrust Reverser Unit

Approved for Public Release. Copyright © 2018 Boeing. All rights reserved.

1 Background & Objectives

1.1 Introduction

The continual drive for increased aircraft fuel efficiency and lower aircraft noise has driven the designs of modern commercial turbofan engines towards higher bypass ratio (BPR) and lower fan pressure ratio (FPR) designs. The state-of-the-art ultra-high BPR, low FPR turbofan engines require a large engine diameter for a given thrust, which increases the contribution of engine and nacelle assembly to the overall drag and weight of the aircraft. For this reason, a tight and efficient integration of the large diameter engine to the airframe is critical in maximizing the performance of the aircraft system.

Boeing Commercial Airplanes (Boeing) is currently designing a compact nacelle structure that optimizes the integration of low FPR (LFPR) turbofan engines, as shown in Figure 1-1. The initial step in this activity is to create an inlet that is shorter than the production inlets used on Boeing 787 aircraft, as shown in Figure 1-2. This technology is aimed for entry into service for the next commercial airplane produced by Boeing, and while the benefit depends on multiple factors, for a twin-engined aircraft a fuel saving in the order of 0.5% is targeted through the nacelle weight and drag reduction provided by this technology. Moreover, use of this technology is key to enabling integration of the afore-mentioned large-diameter advanced LFPR turbofans onto airframes, to realize their 25% sfc improvement potential relative to first generation Trent turbofan engines while minimizing the fuel burn penalties associated with the size and installed interference drag of these types of engine.

The project documented in this report focuses on the experimental demonstration of such a short inlet and benchmarking against a conventional inlet in flight, carried out by Rolls-Royce on their 747 FTB in collaboration with Boeing, following on from a preceding ground test which had focused on static operation in crosswind.

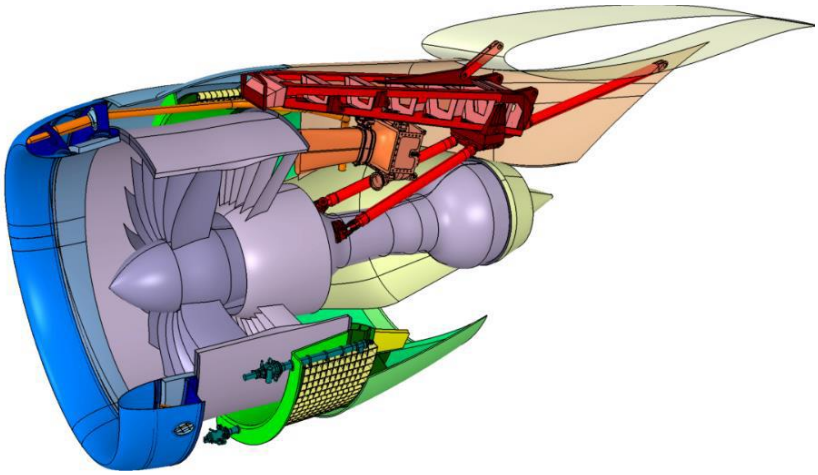

Figure 1-1. Compact Nacelle Concept

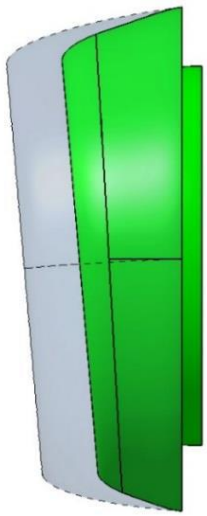

Figure 1-2. Production and short inlet comparison

Approved for Public Release. Copyright © 2018 Boeing. All rights reserved.

1.2 The Short Inlet Collaboration

To ensure the maximum benefit from a short inlet on a future engine and airplane, and to minimize detrimental impacts to engine performance, it is critical to understand the performance coupling between the short inlet and the next generation LFPR engine. Boeing and Rolls-Royce have collaborated on this project to leverage each company's expertise in inlet design, airplane/engine integration, and engine/fan blade design.

The CLEEN II short inlet collaborative research project scope entails design and testing of a Trent 1000 engine-based short inlet in critical ground (static operation in crosswind) and flight conditions (take-off, the low speed high AoA regime, and top-of-climb/cruise), and comparison of its performance against a baseline inlet which has the same aerolines as the Boeing 787 production-standard Trent 1000 engine inlet. The short and baseline inlets are illustrated in **Error! Reference source not found.**.

The goal of this endeavor was to demonstrate the viability of short inlet technologies for future applications and obtain high quality data within a design space encompassing short inlets, to calibrate Boeing and Rolls-Royce design and analytical tools and methods. The detailed design and build of the inlet also served to provide insight to future integration issues of the short inlet hardware. Boeing provided the inlet test hardware and Rolls-Royce provided test facilities, flying test bed aircraft, engine hardware, and engine instrumentation.

The collaboration comprises three phases:

- Phase I, completed in 2016 under the Boeing FAA CLEEN II program, involved feasibility studies and short inlet design and preliminary analytical evaluation.
- Phase II involved ground testing the short and baseline inlets in crosswind and was completed in the winter of 2018 (under the Boeing FAA CLEEN II program), at the Rolls-Royce Crosswind Test Facility, located on the grounds of the NASA John C. Stennis Space Center. The inlets were successfully tested in crosswinds ranging between 20 to 40 Knots as well as 22 and 32 Knot rear-quartering cross-/tailwinds, at three different levels of ground clearance.
  From the perspective of aerodynamic performance, the short inlet performed to design intent. An increase in fan face total pressure distortion was observed at the lowest ground clearance tested. The fan remained free of any instabilities at all conditions.
  Fan blade vibration resonances across a range of engine speeds and flow regimes were generally not significantly influenced by the difference between the short inlet and the baseline inlet. In most cases, the differences in measured fan vibration levels between the baseline and short inlet were within typical test-to-test day data variability.
- Phase III, the culmination of this project and the subject of the present report, involved the flight testing of both inlets on the Rolls-Royce FTB, completed in the summer of 2022, under the Rolls-Royce FAA CLEEN II program.

Approved for Public Release. Copyright © 2018 Boeing. All rights reserved.

2 Apparatus

2.1 The Short and Baseline Inlets

As mentioned in Section 1.2, two inlets were tested during this flight test campaign: the baseline and short inlets, shown in Figure 2-1.

The baseline inlet has the same aerolines as a Boeing 787 production standard Trent 1000 inlet but a novel double skin acoustic barrel and was previously used in the EcoDemonstrator research project. For the needs of the short inlet comparative test campaign, it was modified to incorporate instrumentation such as total pressure rakes and static pressure taps along multiple streamwise cuts, and circumferential stations. This instrumentation is routed via disconnect panels on the rear bulkhead of the inlet to pressure scanners and dynamic signal amplifiers mounted underneath the engine fan case.

The short inlet was a bespoke unit designed and built by Boeing specifically for this research project. The inlet incorporates static pressure taps in streamwise cuts, as well as in circumferential stations, like the instrumented baseline inlet. It was also designed to incorporate the same total pressure rakes used in the baseline inlet. As an experimental piece of hardware, this inlet has a composite skin with no provision for nacelle anti-icing (NAI) or acoustic lining. Instrumentation was again routed via disconnect panels on the rear bulkhead to the scanners and amplifiers on the engine.

The short inlet length is approximately 30% shorter than the baseline inlet. The short inlet is sized for a conventional Trent 1000 fan. It also features similar droop and scarf angles to the conventional baseline inlet. As a result, the bottom dead center section of this inlet is very short and provides little to no local flow diffusion. Externally, the short inlet meets the existing Trent 1000 nacelle aerolines at the fan cowl doors. A comparison of the two inlets as installed in profile, illustrating the transition between short inlet external aerolines and the standard Trent 1000-TEN nacelle can be seen in Figure 2-3.

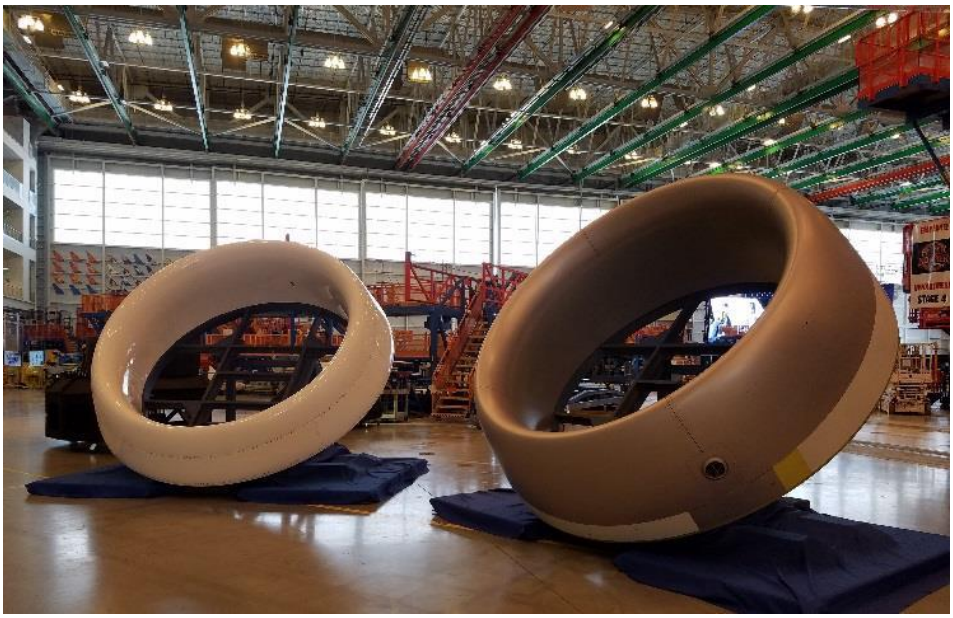

Figure 2-1. Short (left) and baseline (right) inlet hardware

Approved for Public Release. Copyright © 2018 Boeing. All rights reserved.

2.2 Test Vehicle

The engine used for this test was a Trent 1000-TEN engine, Vehicle no. 11100 Build 1. The engine, previously used in other tests, had a significant amount of instrumentation already installed, including modifications to the fan case to accommodate dynamic pressure transducers and a strain-gauged fan set with an integrated telemetry system fitted inside the spinner. The NAI ducting was blanked for the purposes of this campaign. A modified Thrust Reverser Unit (TRU) was used, one specially adapted to accommodate total pressure rakes in the bypass duct, but otherwise to Trent 1000-TEN production standard.

2.3 FTB Installation

The test vehicle was installed in the no. 2 position on the Rolls-Royce Flying Test Bed, a Modified 747-200 (registration number N787RR) which has been previously used extensively for Trent 1000 engine flight testing, including both Trent 1000 Package A and Package B variant 14CFR Part 25 certification high angle-of-attack inlet distortion testing (in 2007 and 2010 respectively), with those test vehicles installed on the aircraft in the same fashion. The non-dimensional ground clearance of the engine depended on the fuel load of the aircraft but was in a similar range to typical ground clearances for a Trent 1000 installed on a Boeing 787 aircraft, and slightly higher than the highest ground clearance tested during the Phase II crosswind test campaign in the Stennis Space Center. The installation can be seen in Figure 2-2 and Figure 2-3.

The same Boeing proprietary algorithm used to calculate angle of attack relative to the inlet centerline axis based on aircraft primary air data during the previous Trent 1000 inlet distortion certification flight tests was reused for both the short and baseline inlet in this flight test campaign.

Figure 2-2 The FTB with the test vehicle in the no. 2 position

Approved for Public Release. Copyright © 2018 Boeing. All rights reserved.

Figure 2-3 Side view comparison of Short (top) and Baseline (bottom) inlets installed on the FTB

Approved for Public Release. Copyright © 2018 Boeing. All rights reserved.

2.4 Instrumentation

Twelve circumferentially equi-spaced rakes were installed in the diffuser section of both inlets, approximately 10” forward of the fan case front flange, recreating the arrangement used during Phase II crosswind testing in Stennis. Only six of these rakes were ‘live’ during the flight test campaign, while the rest were simply ‘dummy’ rakes, installed to maintain the wake patterns presented to the fan during the previous Phase II testing. All twelve rakes were strain-gauged for safety monitoring throughout the test campaign. The six fully functional rakes were the ones closest to top and bottom dead center, the two rakes either side of the rake closest to bottom dead center and the two rakes closest to the inboard (starboard) and outboard (port) sidelines of the inlet. The arrangement of rakes as installed in both inlets can be seen in Figure 2-4.

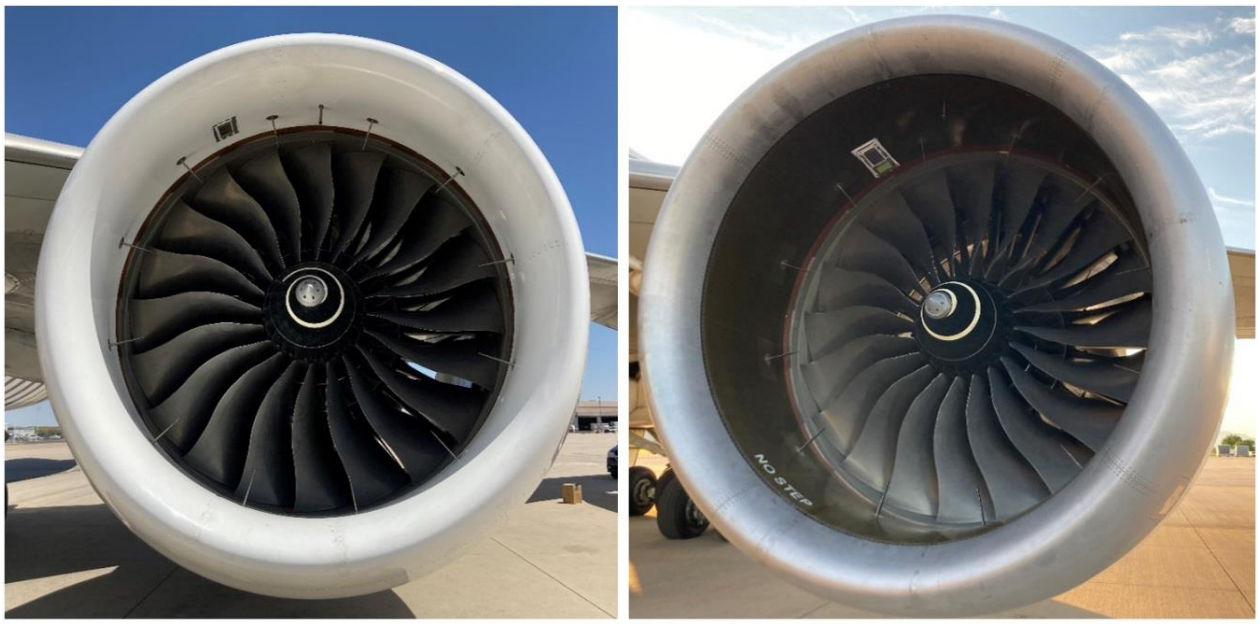

Figure 2-4 Front view of Short (left) and Baseline (right) inlets showing the rakes, metal spinner tip telemetry transmitter, telemetry receiver aerial at 11 o’clock and P2T probe at 12 o’clock.

Each rake is approximately 9” tall and features a combination of simple pitots intended to capture the radial total pressure profiles from the near the intake wall to the rake tip, dynamic pressure transducer (Kulite) pitot probes, and angularity probes. A close-up of an inlet rake, showing the probes in detail, can be seen in Figure 2-5.

A wall static pressure tapping was included next to each rake, on the same axial plane as the rake pitots. All twelve of these circumferential belt static pressure tappings were active during the test campaign.

In addition, both the short and baseline inlet featured axial arrays of static pressure tappings extending from the back end of the diffuser all the way to the inlet leading edge, with a few tappings even placed on the external surface of the inlet, close to the leading edge. The axial arrays were at top and bottom dead center and on the inboard off-keel 7 o’clock position looking into the engine. Close-coupled to six of these static pressure tappings on each axial row were inlet lip surface-mounted dynamic pressure transducers (kulites). Lower inlet quadrant axial arrays of static pressure tappings and kulites are visible in Figure 2-6.

Approved for Public Release. Copyright © 2018 Boeing. All rights reserved.

Figure 2-5 Close-up of an inlet rake

A circumferential array of six equi-spaced dynamic pressure transducers was installed in the forward edge of the engine fan case.

The fan blades were strain-gauged, with a battery powered telemetry transmitter installed in the spinner sending strain gauge signals to a fixed receiver antenna mounted in each inlet. The standard Trent 1000 P2T2 probe was installed in both inlets and active throughout the campaign. These features can be seen in Figure 2-4.

A rearwards-looking camera installed in one of the windows on the port side of the first-class cabin in the main deck of the aircraft afforded a view looking into the engine from the front and slightly above. Video recording was on for all engine running.

Approved for Public Release. Copyright © 2018 Boeing. All rights reserved.

Figure 2-6 Close-up of axial arrays of static pressure tappings and kulites on the short (left) and baseline (right) inlets.

In the TRU, eight rakes were installed in the Trent 1000 nozzle charging plane, each mounted to the inner annulus surface of the bypass duct with the rake tips extending outwards nearly up to the outer annulus. Each rake has an arrangement of pitot probes on it, distributed from very near the inner wall to the rake tip. Static pressure tappings were also distributed close to the rakes on the inner annulus walls, on the same axial plane as the rake pitot probes. A detail of the by-pass rake instrumentation can be seen in Figure 2-7. The fan OGVs were not instrumented in this flight test campaign.

All data acquisition systems on the aircraft were synchronized to IRIG time.

Figure 2-7 By-pass duct rakes

Approved for Public Release. Copyright © 2018 Boeing. All rights reserved.

3 Target Test Points and Overview of Test Flights

3.1 Test Points of Interest

One of the key objectives of the flight test campaign was to determine the effect of inlet distortion on fan vibration, in the context of demonstrating and de-risking short inlet technology in flight. There are two types of fan vibration responses which are of interest here: first engine order (1EO), off-resonant response; and resonant responses.

1EO forcing produced by the inlet is particularly high in almost all high-speed flight operations. In conditions where the aircraft pitch angle is high, for example, during take-off rotation, or close to aircraft stall, flow enters the engine at a high AoA with significantly increased non-uniformity and hence produces 1EO forcing on fan blades.

Resonance occurs when the frequency of an excitation matches a natural frequency of the fan blade. The frequency of excitation is produced by a spatially harmonic distortion field that the fan blades pass through during each rotation of the fan. These distortions can be produced by a range of operating conditions, including high angle of attack, crosswind, or when a ground vortex is present. Flow separation in the inlet can be a key driver for the presence of such a harmonic distortion field. There three resonance modes of interest in this flight campaign: these were 2F3EO, 3F6EO and 1T4EO (the names are explained in the page 5 acronym list).

High quality fan vibration and inlet aerodynamic measurements, and back-to-back comparisons between the short and baseline inlets were sought in a range of flight conditions. There were three main flight regimes of interest and within each one of those, critical elements of inlet aerodynamic performance and engine compatibility, in terms of fan vibration, fan stability, and Low Pressure (LP) system efficiency considerations, had to be measured and compared:

- Take-off

While the inlet flow separation in crosswind tends to clean up rapidly with forward speed, the ground vortex strength tends to increase. Fan blade vibrations, particularly the on-resonance responses, may either decay or amplify during the initial phase of a take-off ground roll depending on the distortion patterns present at the fan face.

In a subsequent phase of the take-off regime, the high static pressure asymmetry at the fan face when the aircraft rotates to lift off the runway increases the 1EO forcing on the fan blades which, as already mentioned, can cause an increase in fan vibration levels.

- Low speed high angle-of-attack conditions

On a civil jet, the highest angles of attack that can be flown can only be encountered in the airspeed regime between low altitude wing stall and the flap retraction corner point. At very high inlet angles of attack, shock-induced flow separation can occur at high engine power on the lower quadrant lip of the inlet. As with high crosswind ground static operation inlet flow separation events, high angle of attack inlet flow separation leads to localized dynamic head loss, i.e. high total pressure distortion, at the fan face, which can increase fan vibration levels and/or affect the aerodynamic stability of the fan. An engine / inlet combination must either be free of separated flow at high angles of attack or tolerant to the degree of separation-induced flow distortion that can be encountered with the high angle-of-attack envelope of the aircraft. Thanks to its high-lift devices, the 747 FTB can reach very high

Approved for Public Release. Copyright © 2018 Boeing. All rights reserved.

angles of attack, meaning that both the baseline and short inlets could be flown beyond the angles of attack where separation occurs. Not only could the performance of the two inlets be compared in terms of their flow separation angles of attack, but the tolerance to separation and the post-separation distortion growth behavior could also be investigated.

High angle of attack test point targets were approached by performing power-on approach to stall maneuvers at 15,500 feet, along with left and right wind-up turn maneuvers at Mn = 0.3 / 15,500 feet and Mn = 0.35 / 19,00 feet.

- High speed and altitude top-of-climb and cruise

In straight and level high speed flight, the fan efficiency can be affected by the level of residual wing upwash at the fan face (manifesting as a left-to-right asymmetric swirl pattern), the magnitude and spatial variation of inlet boundary layer thickness (by implication, the total pressure recovery), and flow diffusion.

The Trent 1000 Package B engine 14 CFR Part 25 787-9 aircraft certification high angle of attack inlet distortion FTB flight test matrix was used as a template to define the test points of the present flight test campaign.

3.2 Overview of achieved flight testing

The essential take-off and cruise test points were completed for both the short and baseline inlet, as was the power-on approach to stall test point in the high inlet AoA regime, in both cases up to and beyond the threshold of inlet flow separation. The short inlet wind-up turns can be compared with the Trent 1000 Package B certification flight test results from 2010, in terms of separation inlet AoA and fan vibration responses.

Ground testing with the short inlet took place in the A-17 runup area of the Tucson International Airport (KTUS) in May and June of 2022. This testing included low ambient wind ground static operation to perform instrumentation check-outs, find the fan stress telemetry channel with the most responsive set of fan blade strain gauges on it, and map out the exact fan mechanical speeds for the resonance modes of interest. An opportunity to carry out ground testing in high natural winds materialized on the 20th of May 2022, when 18 Knot winds, gusting to 24 Knots, were blowing in KTUS. The aircraft was oriented so that wind was coming from the port side, and the crosswind test points were performed. The aircraft was then turned so that its nose was into the wind, and the static operation headwind test points were performed.

The first flight with the short inlet installed on the FTB took place on the 1st of July 2022. An MTO thrust off-resonance take-off was performed from KTUS runway 11L in low ground wind conditions. Some fan resonance mapping to complement the ground measurements was completed flying straight and level at Mn = 0.3 and an altitude of 10,000 feet over Gila Bend before the aircraft returned to base.

The second flight took place on the 21st of July 2022. An on-resonance take-off with a very high mechanical fan speed target was performed from KTUS runway 29R in low ground wind conditions. The aircraft transited to the Mesa Gateway aerodrome (KIWA) to perform the other resonance decay ground rolls and take-offs. A medium target fan speed on-resonance take-off was performed in low ground wind conditions from KIWA runway 30R, before the aircraft returned to base in KTUS.

Approved for Public Release. Copyright © 2018 Boeing. All rights reserved.

The third and final flight of the short inlet took place on the 2nd of August 2022. A high target fan speed on-resonance take-off was performed from KTUS runway 11L in low ground wind conditions. Climb and straight and level cruise test points were performed over Gila Bend, en-route to the W291 range which lies off the coast of Southern California. Once there, the approach to power-on stall and left and right wind-up turn dynamic maneuvers were performed before returning to base.

After the third flight was flown and the completeness of the acquired flight data was confirmed, it was agreed that the essential test points with the short inlet had been achieved. The short inlet was swapped out for the baseline inlet on wing and after the instrumentation was confirmed to be functional, the FTB was ready to resume testing in the beginning of September.

The flight of the baseline inlet on the FTB took place on the 7th of September 2022. An MTO thrust off-resonance take-off was performed from KTUS runway 11L in low ground wind conditions. Climb and straight and level cruise test points were performed en-route to W291 in virtually identical conditions to the short inlet test points. In W291, the power-on approach to stall maneuvers were successfully completed.

4 Flight Test Results

4.1 Ground static crosswind and headwind

Figure 4-1 compares the Amplitude-Frequency (AF) levels under crosswind and headwind conditions, normalized across different test campaigns: the current short inlet flight test; the Phase II ground crosswind test in Stennis in 2018; and a Trent 1000 Pack B certification crosswind test in with the baseline inlet in Stennis in 2010. The AF levels show some level of variability across different test campaigns. It should be noted here that vibration levels are not constant during nominally constant wind conditions and engine speed, but instead fluctuate about a time-mean value. The quoted vibration amplitude here is the maximum response within 1 second during a prolonged dwell on a fan resonance speed.

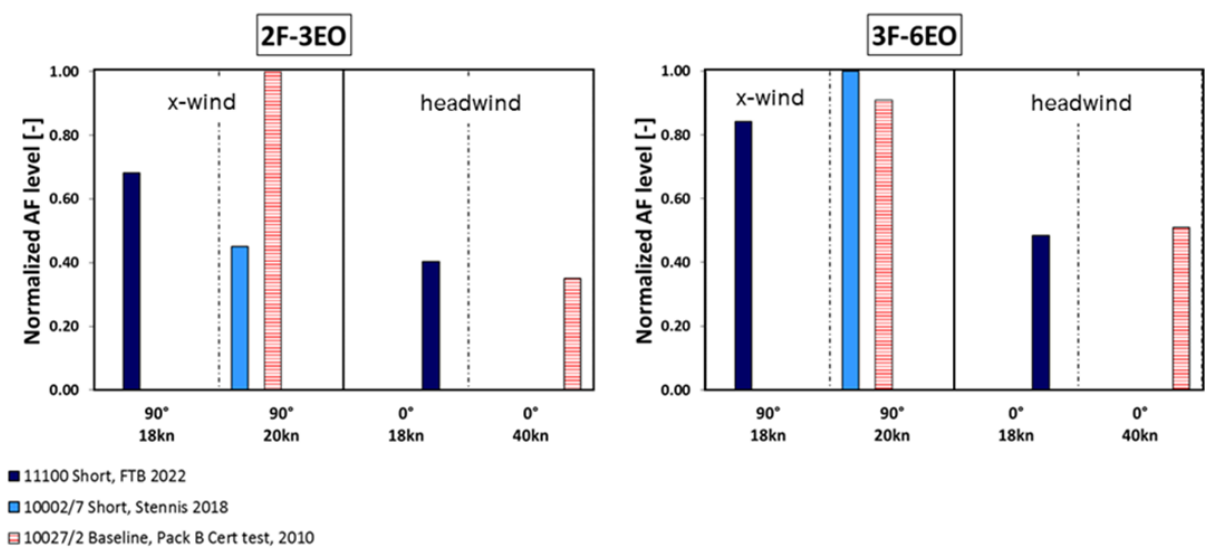

Figure 4-1 Fan responses expressed in AF levels at 2F/3EO and 3F/6EO in ground static crosswind and headwind

Approved for Public Release. Copyright © 2018 Boeing. All rights reserved.

4.2 Take-off rotation

Fan stress and aerodynamic measurements were obtained during an off-resonance MTO ground roll and take-off and three on-resonance ground roll and take-off test points for the short inlet, and an off-resonance MTO ground roll and take-off for the baseline inlet. At the critical lift-off rotation phase of the off-resonance MTO take-offs, where the aircraft pitch angle temporarily reaches high values, a comparison of short and baseline inlet aerodynamic measurements, as shown in Figure 4-3, clearly shows increased levels of top-to-bottom static pressure asymmetry and left-to-right swirl asymmetry in the short inlet, which lead to higher fan forcing relative to the baseline inlet.

Figure 4-2 MTO thrust take-off from Tucson International Airport during the 1st flight of the short inlet on the FTB, 2 July 2022

Figure 4-4 shows a comparison of the vibration level, normalized between the short and baseline inlet, with the peak inlet AoA and N1 speed achieved at lift-off rotation during the off-resonance MTO thrust take-offs. The 1EO response is not a resonant response and is not dependent upon the natural frequency of the fan set. As a result, the operating point at which the peak 1EO response occurs differs depending on the inlet, and for this assessment, the peak value for 1F/1EO is taken for comparison purposes. The vibration levels are expressed as normalized AF. As can be seen in Figure 4-4, the 1EO forcing is significantly increased for the short inlet. This is due to the stronger 1EO flow distortion in the short inlet shown in Figure 4-3. However, the fan blade stresses for the short inlet during the MTO take-off maneuver were still well within acceptable limits.

Approved for Public Release. Copyright © 2018 Boeing. All rights reserved.

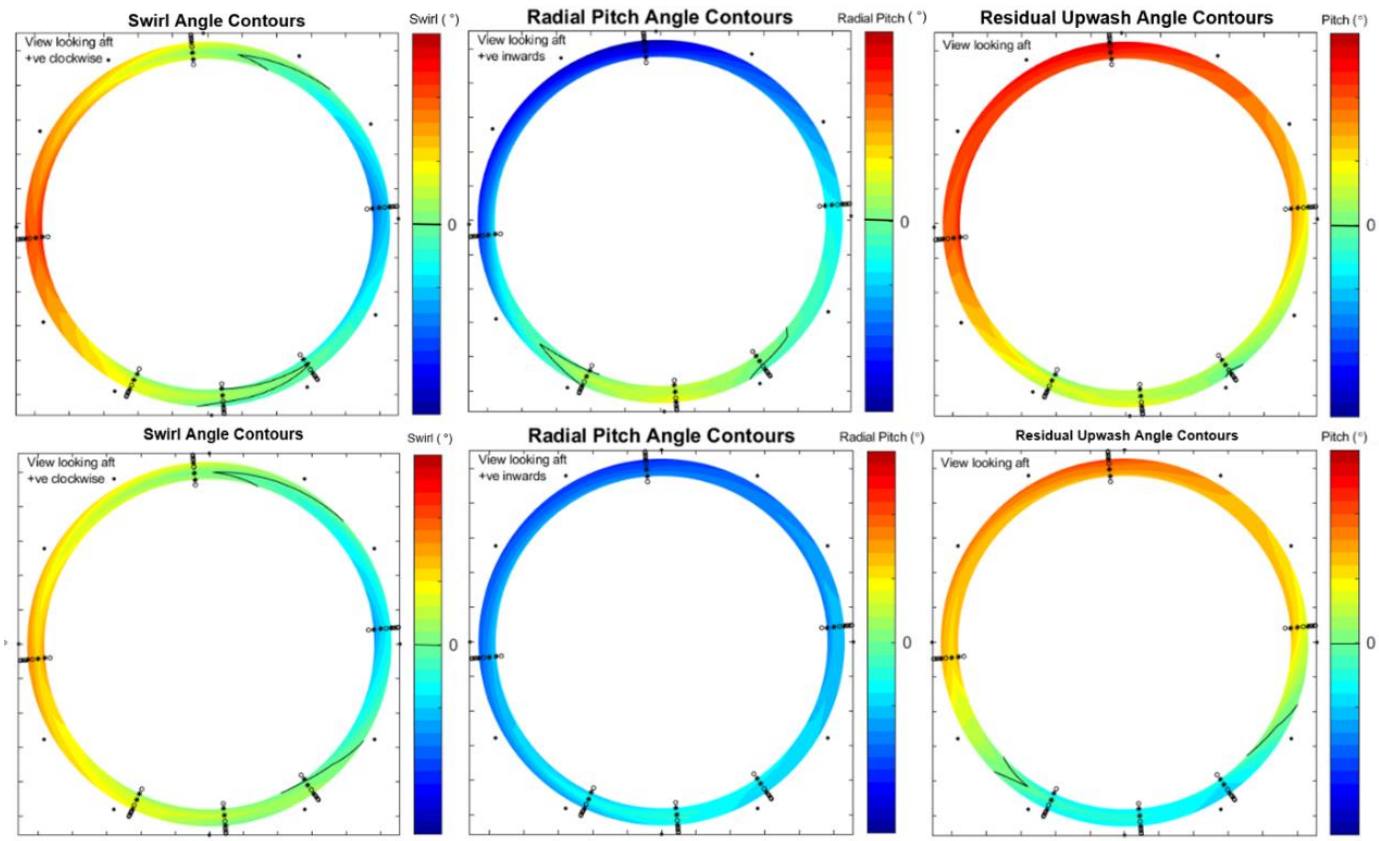

Figure 4-3 Comparison of short (top row) vs baseline inlet (bottom row) MTO thrust take-off test point peak inlet AoA during lift-off rotation measurements

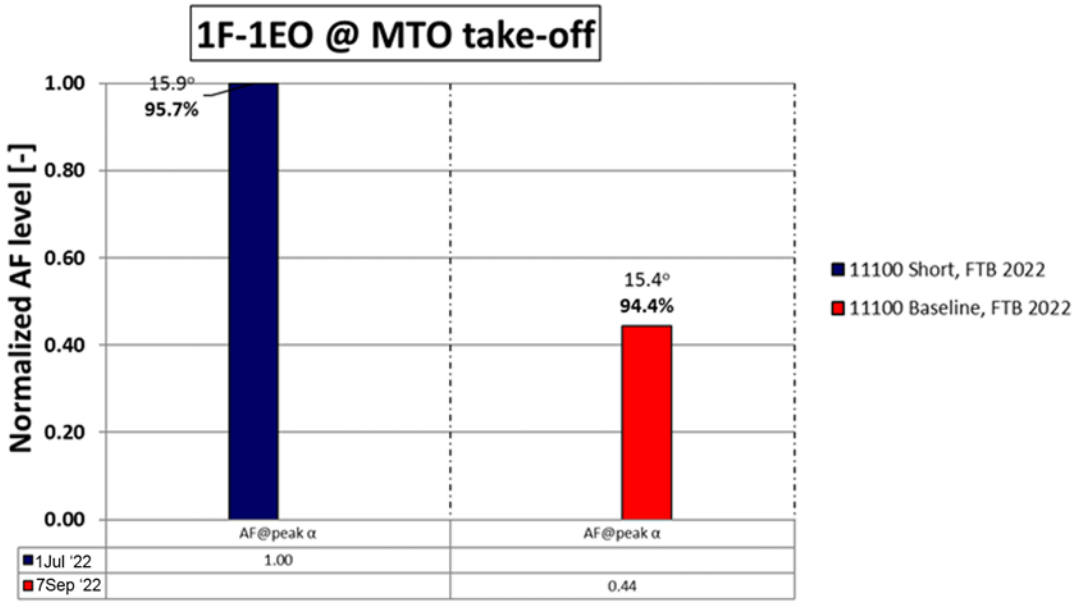

Figure 4-4 Comparison of 1F/1EO response between short and baseline inlet during 74klbf MTO-equivalent take-off rotation

Approved for Public Release. Copyright © 2018 Boeing. All rights reserved.

4.3 High Angle-of-Attack inlet distortion

Inlet flow separation events only occurred at very high inlet AoAs for all the high angle-of-attack test points of the campaign where separation was achieved. The short inlet met and even exceeded expectations of its performance in the high AoA regime, having been flown to the point of flow separation and beyond in all the power-on approach to stall and wind-up turn test points performed. The power-on stall maneuver test points that were also successfully completed with the baseline inlet allow for direct comparisons of aerodynamic instrumentation data with the short inlet measurements and paint a more complete baseline inlet post-separation picture than was ever seen during previous Trent 1000 certification flight tests, where the only meaningful aerodynamic instrumentation in the inlet was an axial array of lip statics at bottom dead center. For wind-up turn maneuvers, the short inlet data can be compared to Trent 1000 Package B certification flight test results from 2010 in terms of inlet flow separation angle of attack and fan vibration responses.

Some of the important findings from the high AoA regime testing are as follows:

- For both the short and baseline inlets, flow separation occurs at lower angles of attack in right wind-up turns than in left wind-up turns, by a margin of approximately 2° inlet AoA. Indeed, it is very difficult to achieve inlet flow separation in left wind-up turns within the AoA envelope of even the 747 FTB, especially for the baseline inlet. This is mostly due to the canted installation of the nacelle, as the pylon is perpendicular to the wing and the wing has some dihedral, and the trend is consistent with observations from previous Trent 1000 certification high AoA flight tests on the FTB. As shown in Figure 4-5 below, even in power-on approach to stall maneuvers, the most highly aerodynamically loaded region of the inlet is at 7 o'clock looking into the engine, and that is where is flow separation will first appear when the separation AoA threshold is reached, unless a significant sideslip component is also present. In a right wind-up turn, this separation pattern is reinforced, whereas in a left wind-up turn it is partially cancelled out by the local flow field.
- The high angle of attack flow separation threshold trends for the short inlet are much closer to the baseline inlet trends than the pre-test isolated CFD predictions had indicated. The difference in flow separation angles of attack is 1° at most. This suggests that there is a flow coupling effect due to the presence of the fan and its proximity to the highly loaded inlet lip section of the short inlet, delaying separation or at least suppressing the separated flow after inlet lip serration has occurred. The extensive pre- and post-separation aerodynamic measurements obtained during the flight test provide a high value dataset to allow the validation of the coupled nacelle / LP system analytical tools that may confirm this effect.

Approved for Public Release. Copyright © 2018 Boeing. All rights reserved.

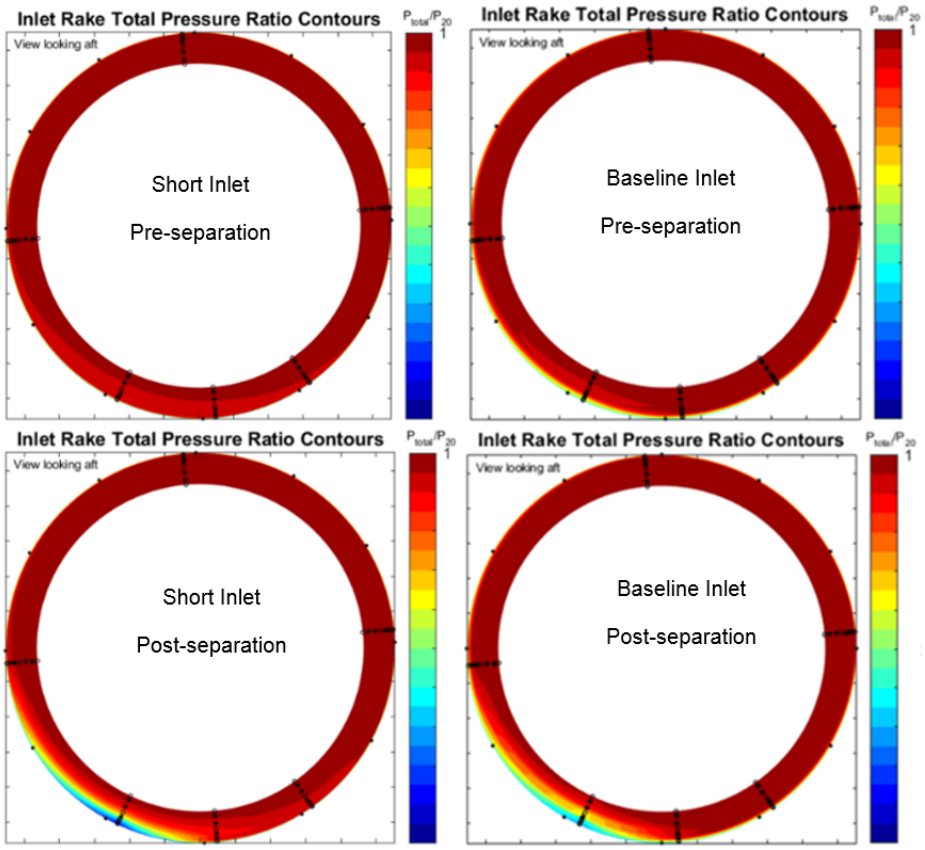

Figure 4-5 Comparison of short and baseline inlet pre- and post-separation inlet rake total pressure contours in the power-on approach to stall max inlet AoA maneuver

Inlet flow separation at high AoA potentially affects the fan vibration amplitudes, both in terms of 1EO and resonant responses. Figure 4-6 shows a comparison of 1F/1EO AF levels normalized between the short and baseline inlets, with the Trent 1000 Package B certification test result also included, during the power-on approach to stall maneuver at 15,500 feet, at the highest inlet AoA achieved in each respective test. Inlet flow separation was present in all three of these instances. It can be seen in Figure 4-6 that the vibration amplitudes are identical between the short and baseline inlet. It should be noted that the vibration level from the most responsive fan blade strain gauge is quoted at the highest AoA for comparison purposes. The current AF levels also show good agreement with the previous certification test result.

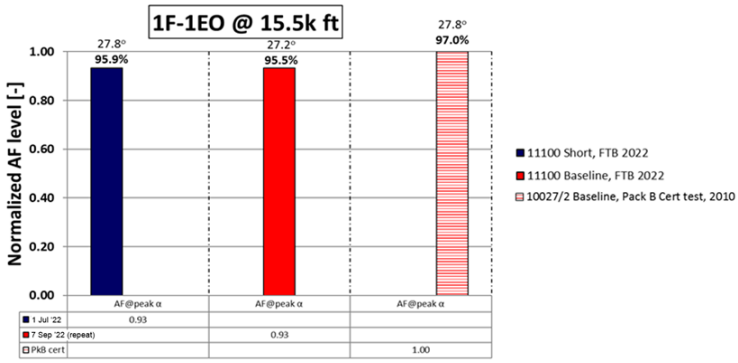

Figure 4-6 Comparison of 1F/1EO responses for short and baseline inlets during power-on approach to stall

Approved for Public Release. Copyright © 2018 Boeing. All rights reserved.

Figure 4-7 compares AF levels normalized at the 1T/4EO crossing during the short inlet left and right wind-up turns at 15,500 feet and Mn = 0.3 to the baseline inlet Trent 1000 Package B certification test right wind-up turn. The short inlet maneuvers were closer to matching the 1T4EO crossing fan resonance speeds than the maneuvers that were previously flown with the baseline inlet. Even so, the vibration levels for the short inlet are significantly lower than for the baseline inlet.

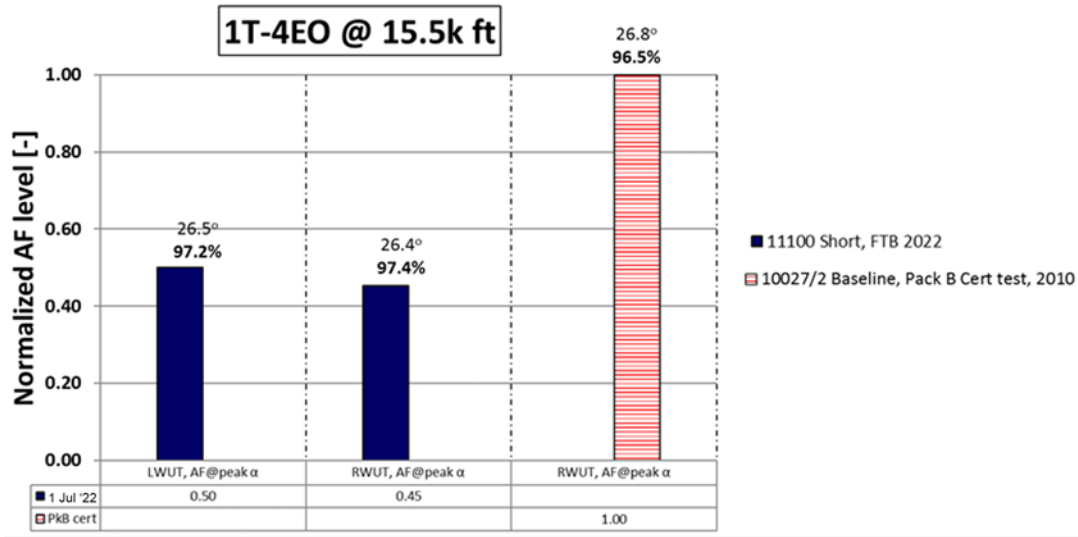

Figure 4-7 Comparison of 1T/4EO response for short and baseline inlet during M = 0.3 wind-up turns at 15,500 feet

4.4 Cruise performance

Measurements were taken in very stable straight and level flight with virtually no perturbations for several minutes, and near-identical flight conditions between the short and baseline inlets. A full set of the desired data was obtained, and comparisons between the short and baseline inlet are illustrated in Figure 4-8, where it can be seen that:

- The short inlet left-to-right swirl asymmetry has nearly twice the magnitude of the baseline inlet asymmetry pattern. Note: the Trent 1000 fan rotates clockwise when seen forward-looking-aft, so co-rotating swirl is plotted as positive.
- The average residual upwash angle in the short inlet is higher than in the baseline inlet. The circumferential variation pattern is broadly similar, but in the short inlet, the absolute pitch angle remains positive everywhere, whereas the pattern appears offset downwards by a few degrees in the baseline inlet, with negative absolute pitch angles in the lower quadrant diffuser section.
- The left-to-right swirl asymmetry and lack of diffusion in the lower quadrant of the short inlet are felt downstream of the fan in the by-pass duct rake total pressure distributions. The observed patterns have implications not only for LP system efficiency, stability margins and forcing, but potentially also on the by-pass duct losses and fan stream exhaust nozzle performance.

It was also found that, as expected:

- The boundary layer thickness at the inlet rake plane is thinner in the short inlet.
- There is more top-to-bottom static pressure asymmetry in the short inlet due to lack of diffusion in the bottom quadrant of this intake.

Approved for Public Release. Copyright © 2018 Boeing. All rights reserved.

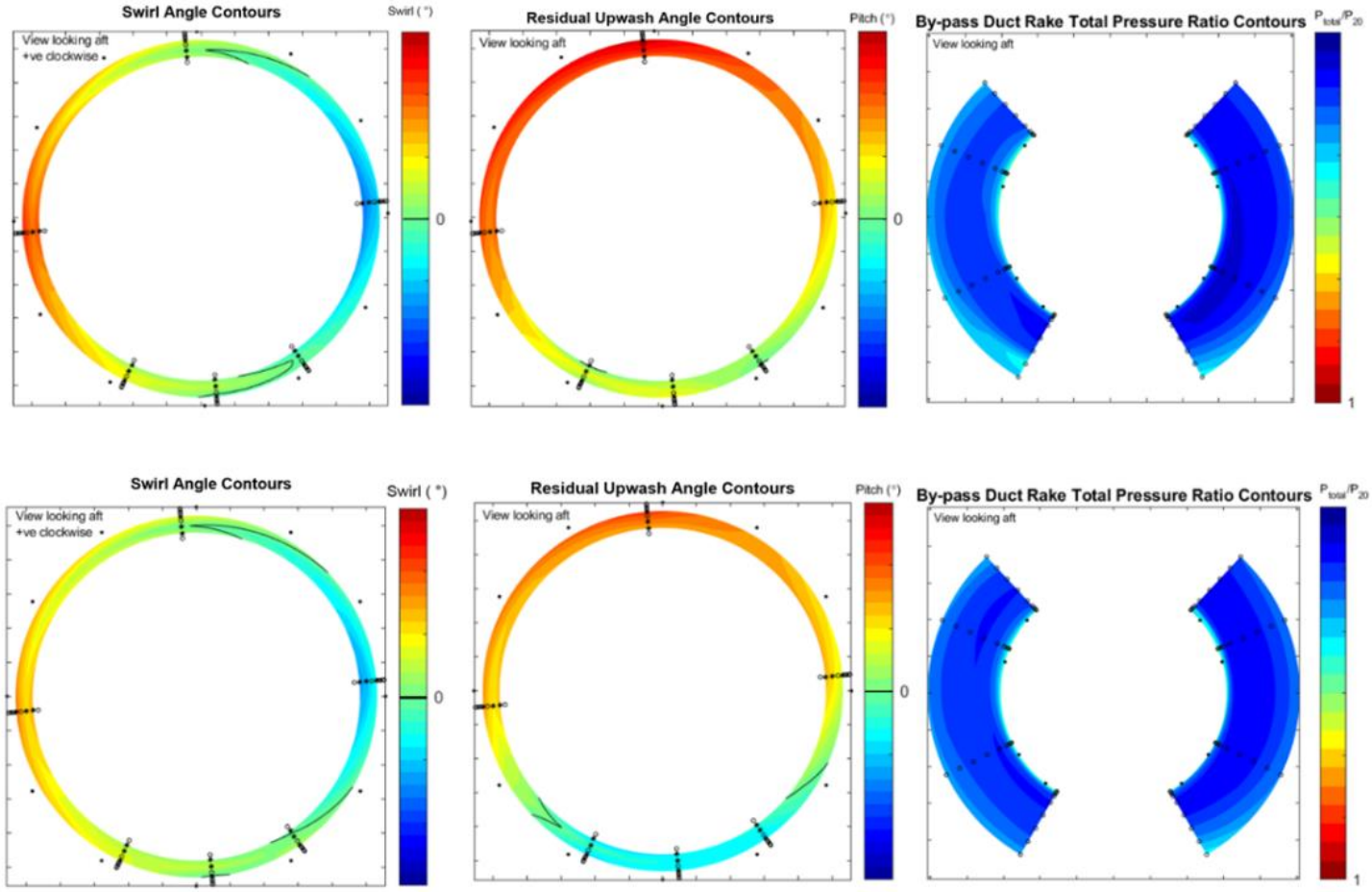

Figure 4-8 Comparison of short (top row) vs baseline (bottom row) inlet cruise test point measurements

Approved for Public Release. Copyright © 2018 Boeing. All rights reserved.

5 Conclusions

Shortening a civil high-BPR turbofan's air inlet by approximately 30% relative to current typical design proportions can yield fuel burn improvements of the order of 0.5% for a twin-engined aircraft through nacelle weight and drag reduction, offset slightly by a reduction in fan efficiency despite an inlet total pressure recovery improvement. Moreover, a shorter inlet can relieve architectural constraints that would otherwise make airframe integration of next generation ultra-high BPR engines challenging, if not impossible. This could allow the potential sfc reduction benefits of such large-diameter LFPR engines to be realized with a minimized aircraft-level fuel burn penalty, particularly if the close-coupled fan/inlet lip interaction effects of short inlets can be exploited to shrink-wrap the nacelle external aerolines around an engine.

In the present flight test campaign, a short inlet was benchmarked against a baseline standard Trent 1000 inlet. The test matrix focused on the phases of flight where inlet performance and interaction with the fan is most critical; i.e. the take-off ground roll and rotation, the low speed and altitude high angle-of-attack envelope, and the high speed top-of-climb and straight-and-level cruise on-design condition.

The short and baseline inlets and the test engine were fitted with instrumentation which offered an unprecedented extent of coverage, ultimately yielding a high-quality dataset of test measurements, successfully captured in all the flight phases of interest. The acquired dataset will be invaluable for the development and calibration of coupled fan-inlet aerodynamic and fan aeromechanical tools and methods, encompassing the short inlet design space.

In terms of the relative aerodynamic performance of the short inlet as tested, the flight test findings revealed increased levels of top-to-bottom static pressure asymmetry and left-to-right swirl compared to the baseline inlet, as well as higher magnitudes of residual upwash at the fan face due to the reduced inlet duct flow settling length. In the high angle-of-attack regime, the inlet flow separation threshold of the short inlet was only slightly lower than that of the baseline inlet, exceeding expectations based on pre-test isolated CFD predictions and indicating that there may indeed be a fan/inlet lip flow interaction effect present. No fan instability was observed even at the highest levels of inlet flow distortion exposure reached in this campaign.

From a fan vibration perspective, a correlation between inlet flow distortion and fan vibration responses was shown in the AF levels for both off- and on-resonance conditions. On-resonance fan blade responses for the short inlet were either similar or less severe than those for the baseline inlet for the three resonance modes of interest. Off-resonance 1EO forcing during take-off rotation was more than double that of the baseline inlet. Although the fan stresses were well within acceptability limits for this blade, the difference is significant, especially in consideration of future fan blade designs.

Despite the non-optimum design attributes of the short inlet as tested, this campaign has demonstrated the viability of short inlet technology at TRL6 level, if only with respect to engine-inlet compatibility at the present time.

Improvements in the design of future short inlets, developed with the aid of the tools that will be refined using the validation dataset acquired during the present test campaign, may alleviate some of the effects of increased flow asymmetry on fan forcing and LP system efficiency.

Approved for Public Release. Copyright © 2018 Boeing. All rights reserved.